A SPECIFIC MAGNITUDE BUDGET FOR THE DETECTION OF 30 NUCLEAR EARTHQUAKES IN URBAN AREAS SUBJECT TO A NATURAL SEISMIC HAZARD.

ALEXIS ZAGANIDIS

Abstract. Multiple underground nuclear explosions may trigger the rupture of seismic faults and mimic a natural earthquake. Moreover, multiple nuclear explosions can be spatially arranged (on a vertical line for instance) and temporally synchronized in order to reduce significantly the P-waves (except inside both spherical cones along the vertical line arrangement). A Specific Magnitude Budget, with the relevant elementary approximations, is relatively enough accurate to compare unambiguously the energy of the stress-drop from the fault rupture and the energy of the radiated seismic waves. Indeed, for the largest natural earthquakes ($M_w \geq 8.0$), we define very conservatively their average seismic radiation efficiency to 0.5. The natural seismic radiation efficiency ranges between 0.124 and 0.569 around the average 0.294 (the natural Specific Magnitude Budget range between $\Delta_{nat}^{min} M_Z = -0.604$ and $\Delta_{nat}^{max} M_Z = -0.163$ around the average $\Delta_{nat}^{mean} M_Z = -0.354$). On the other hand, the nuclear seismic radiation efficiency ranges between 1.297 and 1 218 around the average 95.4 (the nuclear Specific Magnitude Budget range between $\Delta_{nuc}^{min} M_Z = 0.075$ and $\Delta_{nuc}^{max} M_Z = 2.057$ around the average $\Delta_{nuc}^{mean} M_Z = 1.320$). In practice, the natural seismic radiation efficiency is always 2.302× smaller than the nuclear seismic radiation efficiency (an artificial Specific Magnitude Budget gap of $\Delta_{gap} M_Z = 0.241$). Indeed, to provoke a more powerful stress-drop from the fault rupture with multiple underground explosions, an accurate information about the future epicenters should be known which is impossible in practice. Lowering too much the energy of the multiple underground nuclear explosions would also increase the risk of not triggering at all the fault rupture.

A Specific Magnitude Budget for the detection of 30 nuclear earthquakes in urban areas subject to an existing natural seismic hazard is an extremely important research task to do for the nuclear safety of the world.

Elementary approximations in the well established framework of the propagating waves in continuous media are used for the Specific Magnitude Budget in the present article.

1- The Kinetic energy of the propagating waves in continuous media is roughly equal to the Potential energy of that ones.

2- If the seismic station is not far away from the seismic wave source ($\sqrt{x^2 + y^2} < 4 \times h$), the seismic waves come directly from the source itself. The Specific

Date: March 17, 2023.

Energy/Magnitude Budget with this previous hypothesis are the following:

$$R_Z = E_R/E_{Work} = \frac{4\pi}{32} \times C_Z \times \rho \times \overline{PGV}^2 \times d_e^2 \times V_S \times \Delta T_S/E_7$$

(1) $$\times\, exp\left(\bar{\alpha}_S \times d_e/log\left(31.62, e\right)\right)/31.62^{M_{Work}-7}$$

$$\Delta M_Z = log\left(E_R\right) - log E_{Work}$$

(2) $$= log\left(31.62, \frac{4\pi}{32} \times C_Z \times \rho \times \overline{PGV}^2 \times d_e^2 \times V_S \times \Delta T_S/E_7\right)$$

$$+\, \bar{\alpha}_S \times d_e - \left(M_{Work} - 7\right)$$

(3)

where :

(4) $C_Z \cong 1/132.768$

(5) $\rho \cong 2\ 650\ kg/m^2$ $\qquad V_S \cong 4\ 500\ m/s^2$

(6) $E_7 \cong 1.995 \times 10^{15}\ J$ $\qquad \bar{\alpha}_S \cong log\left(31.62, e\right)\dfrac{2\pi \times \bar{f}_S}{Q_S \times V_S}$

(7) $\bar{f}_S \cong 2\ Hz$ $\qquad Q_S \cong 250$

The mechanical magnitude M_{Work} is of the stress-drop from the fault rupture is closely related to the moment magnitude scale M_w (Figure):

$$E_{Work} = \frac{\Delta\sigma\mu\bar{u}S}{G}$$

$$= \frac{\Delta\sigma M_0}{G}$$

$$\cong \frac{\beta\left(SR\right)^{-0.23} M_0}{G}$$

(8) $$10^{1.5M_{Work}} \cong \left(10\right)^{-0.23\times M_w/1.5}\, 10^{1.5M_w}$$

(9) $$M_{Work} \cong 0.898 \times M_w \pm 0.153$$

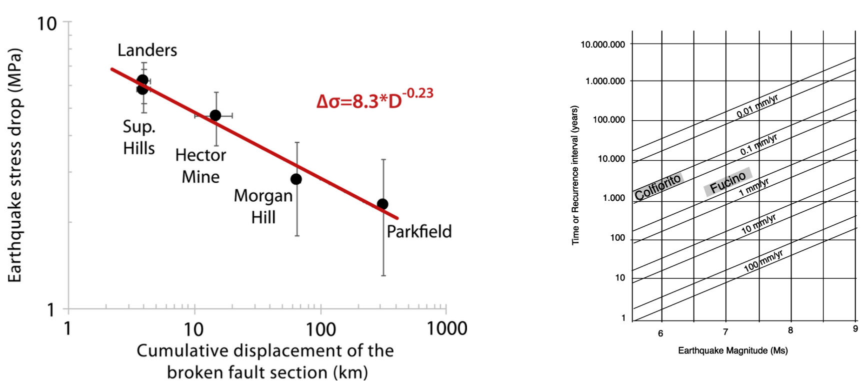

FIGURE 1

The factor 4π is the unit sphere surface. The factor 96 come from a standard seismic radiation efficiency of 1/3, a doubled amplitude of the seismic waves when they reflect to the Earth's surface (factor 2^2), a sin^2 main envelop for the ground velocity (factor 2^2) and a sinusoidal oscillation of the seismic wave (factor 2).

C_Z is a universal constant for every earthquakes. $\overline{PGV}$ is the maximum of the main envelop of the ground velocity at the seismic station. d_e is the effective hypocentral distance depending on the eccentricity of the isoseisms of the shake map ($d_e = d$ for a null eccentricity of the isoseisms of the shake map).

ρ is the density of the rocks at the recording seismic station. V_S is the speed of the S-waves at the recording seismic station. ΔT_S is the time duration of the main envelop of the S-waves. E_7 is the energy of a 7.0 M_w magnitude earthquake. $\bar{f}_S$ is the most representative frequency of the S-Waves. Q_S is the maximal quality factor of the S-waves through the seismic attenuation.

$$x_h = x/h \tag{10}$$

$$y_h = y/h \tag{11}$$

$$l_h = l/h \tag{12}$$

$$f(x_h, y_h, l_h) = \frac{1}{l_h} \int_{-l_h/2}^{+l_h/2} \frac{dx'_h}{(x_h - x'_h)^2 + y_h^2 + 1} \tag{13}$$

$$1/\sqrt{1-e^2} = \frac{a}{b} = \frac{\partial_y^2 f(0,0,l_h)}{\partial_x^2 f(0,0,l_h)} \tag{14}$$

$$d_e = \frac{h}{\sqrt{f(x_h, y_h, l_h)}} \tag{15}$$

x, y, h, l are the coordinates of the seismic station with respect to the isoseisms orientations, the hypocentral depth and the horizontal fault rupture length.

3- If the seismic station is far away from the seismic wave source ($\sqrt{x^2+y^2} > 4 \times h$), the seismic waves are guided between the Earth's surface and the deeper layers of the Earth's crust. We neglect the seismic waves with an upward angle larger than 45° and with a downward angle smaller than 0° because of the seismic attenuation. The Specific Energy/Magnitude Budget with this previous hypothesis are the following:

$$R_Z = E_R/E_{Work} =$$

$$\frac{4\pi\sqrt{2}}{32\left(\sqrt{2}-1\right)} \times C_Z \times \rho \times \overline{PGV}^2 \times d_e \times h \times V_S \times \Delta T_S/E_7$$

$$\times\, exp\left(\alpha_S \times d_e/cos\left(\pi/8\right)/log\left(31.62, e\right)\right)/31.62^{M_{Work}-7} \tag{16}$$

$$\Delta M_Z = log\left(E_R\right) - logE_{Work}$$

$$= log\left(31.62, \frac{4\pi\sqrt{2}}{32\left(\sqrt{2}-1\right)} \times C_Z \times \rho \times \overline{PGV}^2 \times d_e \times h \times V_S \times \Delta T_S/E_7\right) \tag{17}$$

$$+\, \alpha_S \times d_e/cos\left(\pi/8\right) - \left(M_{Work} - 7\right)$$

(18)

where :

$$C_Z \cong 1/132.768 \tag{19}$$

$$\rho \cong 2\ 650\ kg/m^2 \qquad V_S \cong 4\ 500\ m/s^2 \tag{20}$$

$$E_7 \cong 1.995 \times 10^{15}\ J \qquad \bar{\alpha_S} \cong log\left(31.62, e\right)\frac{2\pi \times \bar{f_S}}{Q_S \times V_S} \tag{21}$$

$$\bar{f_S} \cong 2\ Hz \qquad Q_S \cong 250 \tag{22}$$

The factor $\sqrt{2}/\left(\sqrt{2}-1\right)\left(h/d_e\right)$ is the ratio between the cylinder surface of radius d_e and height h and the cone surface with the angle lying between 0° and +45°. For the seismic attenuation, we used the approximate average length path $d_e/cos\left(\pi/8\right)$ with an upward angle of +22.5°.

4- We also used a fitted model for the $\overline{PGV}$ with respect to the $\overline{PGA}$ (Figures 1, 2 and 3).

SHAKING	Not felt	Weak	Light	Moderate	Strong	Very strong	Severe	Violent	Extreme
DAMAGE	None	None	None	Very light	Light	Moderate	Moderate/heavy	Heavy	Very heavy
PGA(%g)	<0.05	0.3	2.76	6.2	11.5	21.5	40.1	74.7	>139
PGV(cm/s)	<0.02	0.13	1.41	4.65	9.64	20	41.4	85.8	>178
INTENSITY	I	II-III	IV	V	VI	VII	VIII	IX	X+

Scale based on Worden et al. (2012) Version 1: Processed 2020-02-06T19:31:16Z
△ Seismic Instrument ○ Reported Intensity ★ Epicenter ▭ Rupture

Figure 2. MMI Legend of Shake Maps.

Wikipedia provide the list of the costliest earthquakes. We add to that list, the earthquakes in San Fernando 1971, in Coalinga 1983, in Borah Peak 1983, in Whittier Narrows 1987, in Landers 1992, in Kushiro 1993, in Geiyo 2001, in Southern Peru 2001, in Kaohsiung 2010, in Chiapas 2017, in Ridgecrest 2019 and in Taitung 2022. We removed from the costliest earthquake list, the earthquakes too far from a reliable recording seismic station. The earthquake in Tangshan 1976 and in San Francisco 1906 have a great historical importance but there are no reliable recording seismic station close to that earthquake. Therefore, we study separately the earthquake in Tangshan 1976 and the earthquake in San Francisco 1906.

We googled "location name + year + ground acceleration" to get the FULL ground acceleration plots of the earthquake. We googled "seismic station name + latitude

FittedModel[$-0.00915972\,x + 1.2185\,x^{1.17218}$]

	Estimate	Standard Error	Confidence Interval
a	−0.00915972	0.219356	{−0.573033, 0.554713}
b	1.2185	0.22029	{0.652222, 1.78477}
c	1.17218	0.03315	{1.08696, 1.25739}

FIGURE 3. Parameters and Confidence interval of the fitted model for the $\overline{PGV}$ with respect to the $\overline{PGA}$

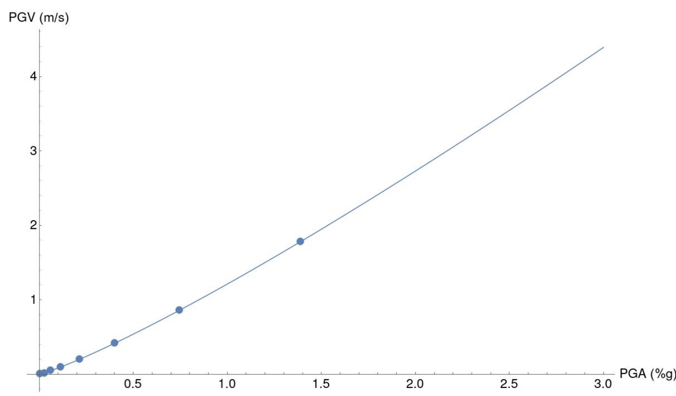

FIGURE 4. Parameters and Confidence interval of the fitted model for the $\overline{PGV}$ with respect to the $\overline{PGA}$

+ longitude" to get the latitude and the longitude of the seismic station corresponding to the ground acceleration plots. The magnitude of the energy of the stress-drop from the fault rupture (M_W), the hypocentral depth, the GPS coordinates of the epicenter, the UTC, the local time and the Shaking Map are given by the corresponding Wikipedia pages.

We define the Specific Magnitude Budget ΔM_Z as the following:

$$\Delta M_Z = log\,(31.62, E_R/E_W) - log\left(31.62, < E_R^{natural}/E_W^{natural} >\right) \tag{23}$$

where

$$< E_R^{natural}/E_W^{natural} > \cong 0.316093 \tag{24}$$

It may be the most useful scientific discovery (differentiating unambiguously nuclear earthquakes to natural earthquakes with a Specific Magnitude Budget ΔM_Z). It was not expected being discovered so late. (Figure 4, 5, 6 and 7).

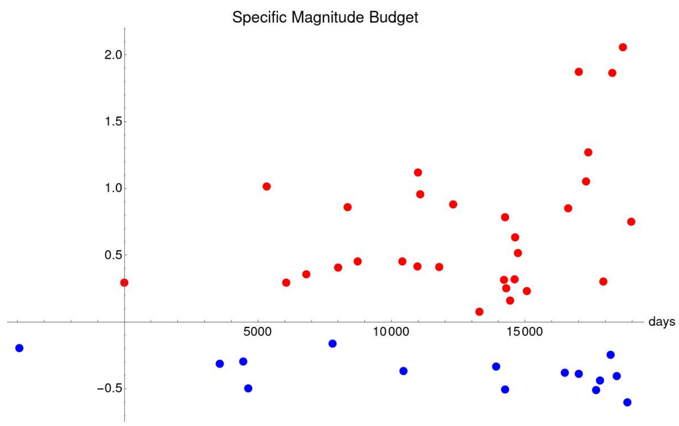

Figure 5. The abscissa is the number of days of the earthquakes from the first nuclear earthquake in San Fernando 1971.

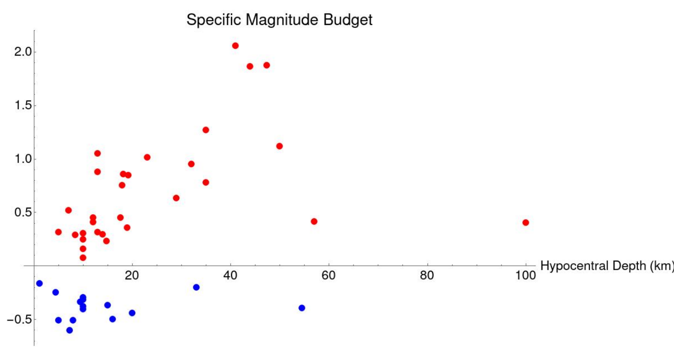

Figure 6. The abscissa is the number of days of the earthquakes from the first nuclear earthquake in San Fernando 1971.

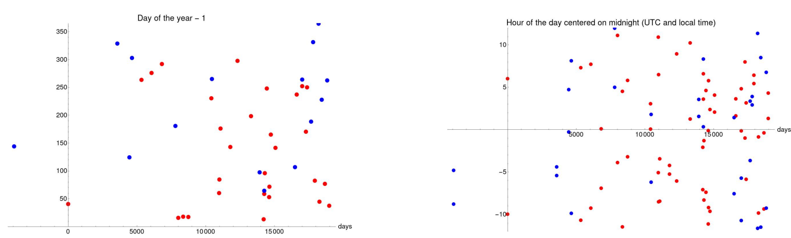

Figure 7. The abscissa is the number of days of the earthquakes from the first nuclear earthquake in San Fernando 1971.

Multiple underground nuclear explosions may trigger the rupture of seismic faults and mimic a natural earthquake. Moreover, multiple nuclear explosions can be spatially arranged (on a vertical line for instance) and temporally synchronized in order to reduce significantly the P-waves (except inside both spherical cones along the vertical line arrangement).

A Specific Magnitude Budget, with the relevant elementary approximations, is relatively enough accurate to compare unambiguously the energy of the stress-drop from the fault rupture and the energy of the radiated seismic waves.

Indeed, for the largest natural earthquakes ($M_w \geq 8.0$), we define very conservatively their average seismic radiation efficiency to 0.5. The natural seismic radiation efficiency ranges between 0.124 and 0.569 around the average 0.294 (the natural Specific Magnitude Budget range between $\Delta_{nat}^{min} M_Z = -0.604$ and $\Delta_{nat}^{max} M_Z = -0.163$ around the average $\Delta_{nat}^{mean} M_Z = -0.354$). On the other hand, the nuclear seismic radiation efficiency ranges between 1.297 and 1 218 around the average 95.4 (the nuclear Specific Magnitude Budget range between $\Delta_{nuc}^{min} M_Z = 0.075$ and $\Delta_{nuc}^{max} M_Z = 2.057$ around the average $\Delta_{nuc}^{mean} M_Z = 1.320$).

In practice, the natural seismic radiation efficiency is always 2.302× smaller than the nuclear seismic radiation efficiency (an artificial Specific Magnitude Budget gap of $\Delta_{gap} M_Z = 0.241$). Indeed, to provoke a more powerful stress-drop from the fault rupture with multiple underground explosions, an accurate information about the future epicenters should be known which is impossible in practice. Lowering too much the energy of the multiple underground nuclear explosions would also increase the risk of not triggering at all the fault rupture.

Japan was hit 10 times, United States were hit 4 times, Mexico was hit 4 times, New Zealand was hit 3 times, Italy was hit 2 times. Peru, Turkey, Croatia, Haiti, Chile, Algeria and Taiwan were hit once time.

The direct costs of the earthquake damages was increased by +340% because of the nuclear earthquakes (1 666 G\$ in total instead of 345 G\$ for the natural earthquakes only). The indirect costs of the more expensive buildings, with respect to the stronger safety standards induced by the 30 nuclear earthquakes, are about 50 000 G\$ over the last 30 years.

There is a year anomaly, the nuclear earthquakes does not occurred on a gap of 80.4 days over 365. The probability of that anomaly is 2.0% about. (The nuclear earthquakes occurred only between the day 12.9 and the day 297.3 of the year with UTC).

There is also a day anomaly, 4 nuclear earthquakes have an UTC or a local time extremely close to midnight. The probability of that anomaly is 1.2% about.

The Energy Budget may have been used incorrectly in the following article: "Observational constraints on the fracture energy of subduction zone earthquakes" written by Venkataraman, Anupama and Kanamori, Hiroo in 2004 (Figure 16).

Characteristic damages of the 30 nuclear earthquakes (Fig. 8, 9, 10, 12, 13 and 14).

A list of comments about the historical political context of the 30 nuclear earthquakes :

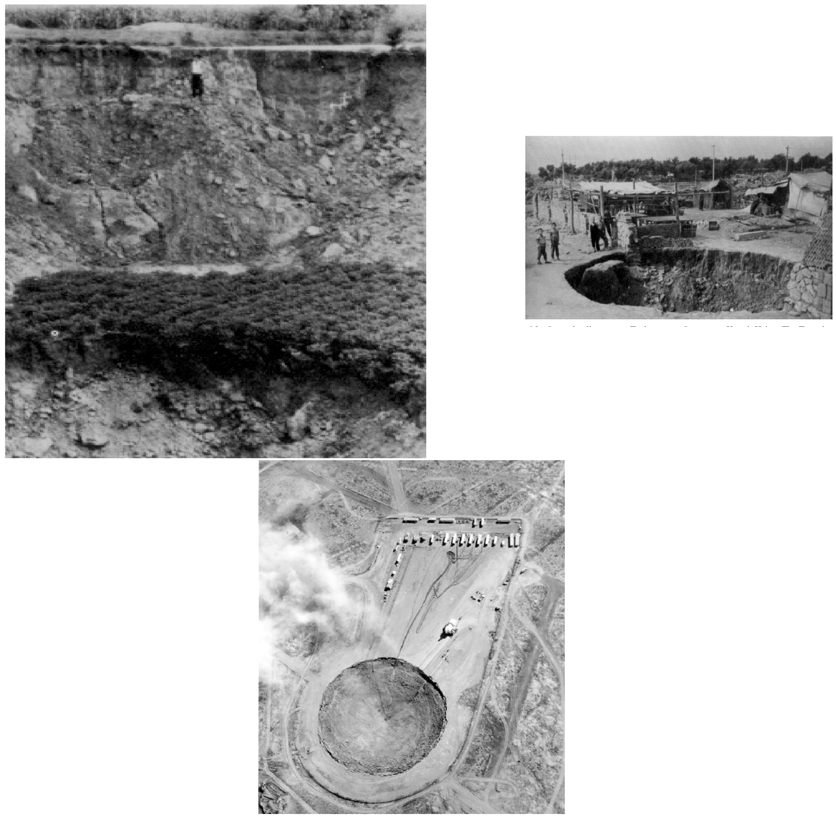

FIGURE 8. Earthquake in Tangshan 1976 and the Nevada test site with underground nuclear tests. The crater in Tangshan 1976 could be a crater from the collapse of a very deep and very large cavity formed by an underground nuclear explosion in Tangshan 1976.

1- The art of terrorism is tenfold : 1) Doing actions that seem impossible to do with catastrophic & strategic consequences, 2) Passing actions off as accidental and/or from external causes, 3) Appearing incompetent/unprofessional and/or Appearing subject to external constraints and/or Appearing suffering from terrorism, 4) Choosing the critical timing, 5) Choosing the critical location, 6) Keeping action information secret and/or spreading popular/viral/confusing/subtle disinformation, 7) Identity change of the terrorist organization and/or disguise the terrorist organization purge as an accidental/natural disaster, 8) Organizing major/spectacular actions that take a lot of investigations resources with minor consequences. 9) Create global disasters that reduce the investigation intelligence, 10) Terrorism by reproducing/amplifying previous known natural disasters to double down the terror about it and complaining about other irrelevant terrorists attacks.

2- The first nuclear earthquake in San Fernando 1971 happened within the Vietnam war context and the Laos war context:

FIGURE 9. Characteristic building damages from a suspected nuclear earthquake in Tangshan 1976 and two other nuclear earthquakes in Northridge 1994 and in Hanshin 1995.

Because of significant logistical stockpiling by PAVN in the Laotian Panhandle, South Vietnam launched Operation Lam Son 719, a military thrust on 8 February 1971. Its goals were to cross into Laos toward the city of Tchepone and cut the Ho Chi Minh Trail, hopefully thwarting a planned North Vietnamese offensive. Aerial support by the U.S. was massive since no American ground units could participate in the operation. On 25 February, PAVN launched a counterattack, and in the face of heavy opposition, the South Vietnamese force withdrew from Laos after losing approximately a third of its men.

The 1971 San Fernando earthquake (also known as the 1971 Sylmar earthquake) occurred in the early morning of February 9 in the foothills of the San Gabriel Mountains in southern California. The event affected a number of health-care facilities in Sylmar, San Fernando, and other densely populated areas north of central Los Angeles. The Olive View Medical Center and Veterans Hospital both experienced very heavy damage, and buildings collapsed at both sites, causing the majority of deaths that occurred. The buildings at both facilities were constructed with mixed styles, but engineers were unable to thoroughly study the buildings' responses because they were not outfitted with instruments for recording strong ground

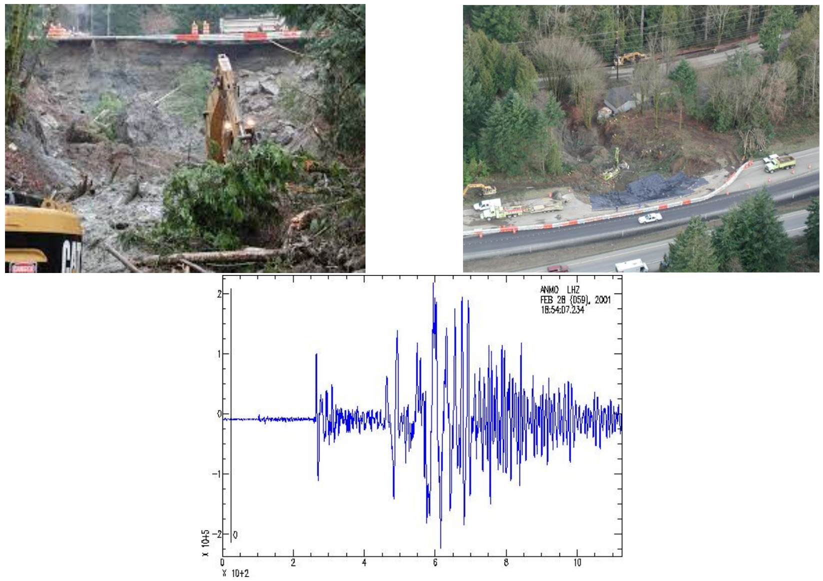

FIGURE 10. It could be a crater from the collapse of a very deep and very large cavity formed by an underground nuclear explosion in Nisqually 2001. Anomalous strong P waves of the 2001 Nisqually earthquake at a distance of 1917 km recorded at the Seismic Station IU ANMO Albuquerque, New Mexico, USA. Since the epicenter was relatively deep (57 km), a smaller nuclear pre-explosions (with a small horizontal alignment) may have been done in order to reduce the first P-waves around the epicenter and the S-waves of the smaller pre-explosions mask the P-waves of the main nuclear explosions (with a vertical line alignment). However, the P-wave of the smaller nuclear pre-explosions are relatively strong far way of the epicenter (horizontal plane) and the seismic attenuation is larger far away for the S-waves than the strong P-waves. Therefore, there is a strong initial peak of the P-waves of the smaller nuclear pre-explosions.

motion, and this prompted the Veterans Administration to later install seismometers at its high-risk sites.

3- With a 90%-95% confidence level, the earthquake in Tangshan 1976 is also a nuclear earthquake with a Specific Energy Budget between $\times 2.17$ - $\times 6.23$ (1-sigma interval about) or a Specific Magnitude Budget ΔM_Z between $\times 0.22$ - $\times 0.53$ (1-sigma interval about).

Like the other 30 nuclear earthquakes, there was a large ratio between the vertical ground acceleration and the horizontal acceleration:

Strong motion records obtained on ground during the main shock in Tangshan 1976 show a rather strong vertical component, with max. vertical acceleration about 50%-100% of that of the horizontal even at epicenter

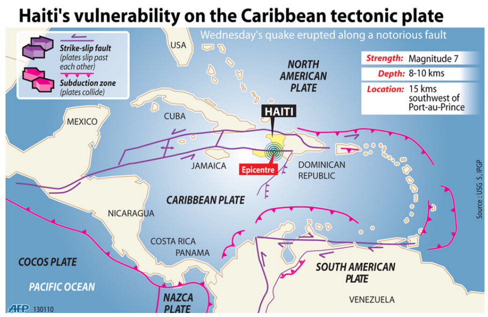

FIGURE 11. Port-au-Prince is located inside a double seismic strike-slip fault system. Therefore, the stress energy accumulated in that seismic system is released more easily and more frequently BUT at a lower level. Therefore, it is very unlikely that there will be an earthquake as strong as the one that hit Port-au-Prince in 2010.

distance more than 100 km, and a long duration nearly 100 seconds at that distance.

Like the other 30 nuclear earthquakes, there was that characteristic infrastructure damage at the Figure 10 of the page 17 of the article "1976 Tangshan, China Earthquake" written by J .A. Blume.

4- Very probably, that giant removal was done for of a giant top secret military nuclear subterrene program in Russia : Khrushchev withdrew 1,400 Soviet technicians from the PRC, which canceled some 200 joint scientific projects. In response, Mao justified his belief that Khrushchev had somehow caused China's great economic failures and the famines that occurred in the period of the Great Leap Forward.

5- The soviet propaganda about the Kola Superdeep Borehole was intended to give the impression that there were completely abnormal, mysterious and unknown phenomena at depths beyond 8 km. The soviet propaganda was also intended to give the impression it was much harder or extremely hard to reach depths beyond 8 km. The official drilling of the the Kola Superdeep Borehole started less than a year before the first nuclear earthquake in San Fernando 1971.

6- April 29 1976 – Sino-Soviet split: A concealed bomb explodes at the gates of the Soviet embassy in China, killing four Chinese.The targets were embassy employees, returning from lunch, but on this day they had returned to the embassy earlier. That event took place exactly 3 months before the suspected nuclear earthquake in Tangshan 1976.

7- ONLY 4 days after the USSR made the big Helsinki Accords with the western countries, the worst 1975 Banqiao Dam failure in human history

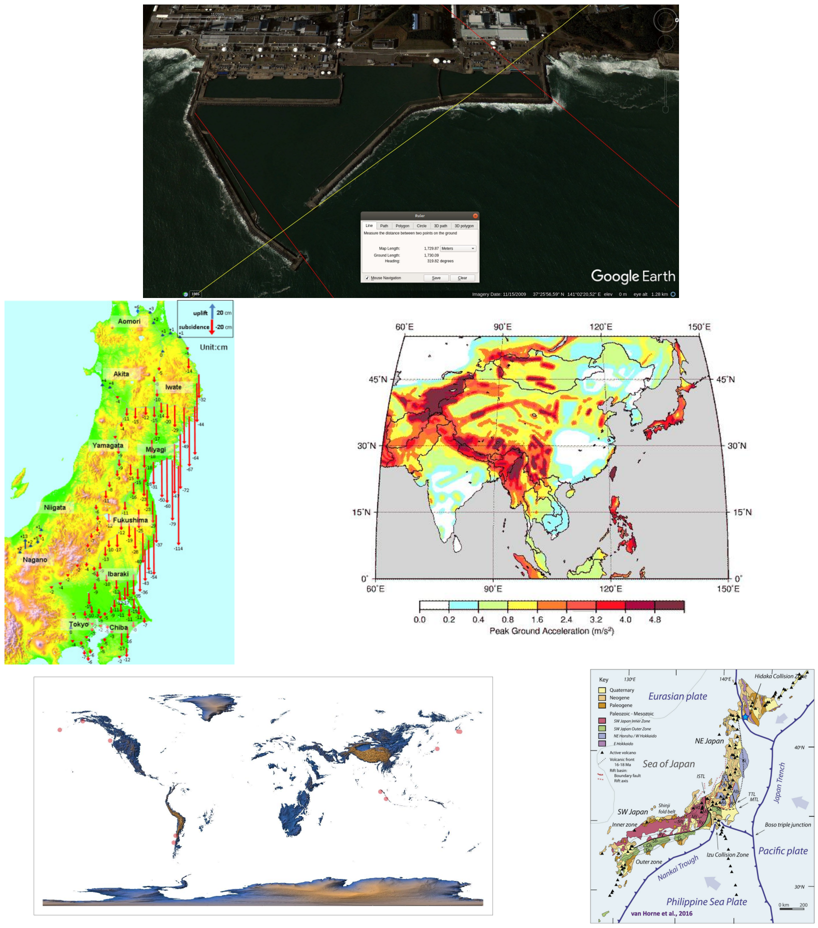

FIGURE 12. The Fukushima Daiichi nuclear disaster was DESIGNED? It was the only nuclear plant with a concave sea wall instead of having a convex sea walls like the Fukushima Daini nuclear plant. The tsunami direction had exactly the right angle (oblique angle of 40° counterclockwise) to lean on the sea wall of the reactors 5 & 6 and being redirected to the reactors 1 & 2 & 3 & 4 at a perpendicular angle with the concave sea wall. Moreover, there is only 0.6% probability to have so many M_w 9.1 earthquakes the last 70 years with respect to the 450 years earlier. Secondly, the other historically known M_w 9.1 earthquakes only happened near high mountain chains arranged in double lines unlike the 2011 Tōhoku earthquake not near from any high mountains. Thirdly, the fault bends significantly 212 km northwest of the epicenter and makes a complete fault rupture almost impossible as required for a 9.1 M_w earthquake. Finally, the Okhotsk plate subsided instead of uplifting as it would be expected for an Oceanic Subduction Zone.

occurred. Few weeks before the nuclear earthquake in Turkey-Syria 2023:

Figure 13. The natural earthquake in San Francisco 1906, the nuclear earthquake in Tangshan 1976 and the nuclear earthquake in Turkey–Syria 2023 have overturned few trains. HOWEVER, the train overturned by a natural earthquake in 1906 was ON the San Andreas fault.

Figure 14. The 2023 Turkey-Syria earthquake created a canyon 35 meters deep and 200 meters wide. It could be a land subsidence from the collapse of a very deep and very large cavity formed by an underground nuclear explosion.

Ankara asked Damascus in Moscow to recognise the YPG as a "terrorist" organisation. 2 months before that nuclear earthquake: Turkey has threatened to send group troops into northeastern Syria in retaliation for a deadly Istanbul bombing on November 13 that President Recep Tayyip Erdogan attributes to the Syrian Kurdish YPG (strongly supported by the the

Turkish Marxist-Leninist Communist Party). Dugin killed his own journalist daughter to keep some secrets about Sars-Cov-2 or nuclear earthquakes?

8- The 11/09/2001 attacks in New York City occurred EXACTLY 30 years after the death of Nikita Sergeyevich Khrushchev. The Gyrotron, the Kola Superdeep Borehole, the Soviet space program, the nuclear Kyshtym disaster, the Cuban Missile Crisis and the Sino-Soviet split started under the Khrushchev's leadership or very soon after it (Figure 15). Napoleon, Mussolini, Kructhnev, Medvedev and Putin may had the Napoleon-complex: little men may try to compensate a lack of physical strength by displaying an extreme drive, ambition, and self-confidence (Figure 15). The Napoleon-complex suggests that shorter men are more likely to have megalomania feelings, initiate conflicts more frequently and respond aggressively to any threat or provocation. Khrushchev was one of the most watched and isolated rulers during his whole retirement. Khrushchev was almost under a regime of semi-liberty during his whole retirement. Probably, that forced and watched isolation during the Khrushchev's retirement was the consequence of a giant top secret military nuclear subterrene program (responsible of the nuclear Kyshtym disaster? The Cuban Missile Crisis was made as a distraction for USA?).

9- The Kaprun disaster was a fire that occurred in an ascending train in the tunnel of the Gletscherbahn Kaprun 2 funicular in Kaprun, Austria, on 11/11/ 2000. The disaster killed 155 people. The inquest ends on September 6, 2001. The 11/09/2001 attacks in New York City. The 04/10/2001, a soviet S-200 missile shot down a commercial plane above the black sea, most of the passengers were Israelis visiting their relatives in Russia. The Tohoku nuclear earthquake the 11/03/2011.

10- 222 days after Russia has Declared Greece "Unfriendly" Country the 22th July 2022, Greece experienced their worst train crash. The worst Greek train crash happened just before the Greek General Elections and the train was completely filled with young graduates. Safety standards were always low in Greece the last 60 years BUT Greece was never in the sights of a very sophisticated terrorist state until very recently. On the night of 29/10/2022, a crowd crush occurred during Halloween festivities in the Itaewon neighborhood of Seoul, South Korea.

11- Earthquake in Tangshan 1976 and the Nevada test site with underground nuclear tests. The crater in Tangshan 1976 could be a crater from the collapse of a very deep and very large cavity formed by an underground nuclear explosion in Tangshan 1976 (Figure 8).

12- Characteristic building damages from a suspected nuclear earthquake in Tangshan 1976 and two other nuclear earthquakes in Northridge 1994 and in Hanshin 1995 (Figure 9).

13- It could be a crater from the collapse of a very deep and very large cavity formed by an underground nuclear explosion in Nisqually 2001 (Figure 10). Anomalous strong P waves of the 2001 Nisqually earthquake at a distance of 1917 km recorded at the Seismic Station IU ANMO Albuquerque, New Mexico, USA (Figure 10). Since the epicenter was relatively deep (57 km), a smaller nuclear pre-explosions (with a small horizontal alignment) may have been done in order to reduce the first P-waves around the epicenter and the S-waves of the smaller pre-explosions mask the P-waves of the main nuclear explosions (with a vertical line alignment). However, the P-wave of the smaller nuclear pre-explosions are relatively strong far way of the epicenter (horizontal plane) and the seismic attenuation is larger far away for the S-waves than the strong P-waves. Therefore, there is a strong initial peak of the P-waves of the smaller nuclear pre-explosions (Figure 10).

14- Port-au-Prince is located inside a double seismic strike-slip fault system. Therefore, the stress energy accumulated in that seismic system is released more easily and more frequently BUT at a lower level. Therefore, it is very unlikely that there will be an earthquake as strong as the one that hit Port-au-Prince in 2010 (Figure 11).

15- The Fukushima Daiichi nuclear disaster was DESIGNED? It was the only nuclear plant with a concave sea wall instead of having a convex sea walls like the Fukushima Daini nuclear plant. The tsunami direction had exactly the right angle (oblique angle of 40° counterclockwise) to lean on the sea wall of the reactors 5 & 6 and being redirected to the reactors 1 & 2 & 3 & 4 at a perpendicular angle with the concave sea wall (Figure 12). Moreover, there is only 0.6% probability to have so many M_w 9.1 earthquakes the last 70 years with respect to the 450 years earlier (Figure 12). Secondly, the other historically known M_w 9.1 earthquakes only happened near high mountain chains arranged in double lines unlike the 2011 Tōhoku earthquake not near from any high mountains (Figure 8). Thirdly, the fault bends significantly 212 km northwest of the epicenter and makes a complete fault rupture almost impossible as required for a 9.1 M_w earthquake (Figure 12). Finally, the Okhotsk plate subsided instead of uplifting as it would be expected for an Oceanic Subduction Zone (Figure 12).

16- The weight of the multiple nuclear H-bombs in Tohoku 2011 is roughly the weight of the Saturn V rocket:

$$\begin{aligned} &r_H \\ &\cong (17.59)/(6.015122 + 2.014101)/931.49 \times 9\ 000 \times 10^{16} \\ &\cong 2.117 \times 10^{17}\ J/ton \end{aligned} \tag{25}$$

$$\begin{aligned} &M_H \\ &\cong 1\ 995 \times 10^{12}/C_Z \times R_Z/(50\%\ r_H) \\ &\cong 3\ 048\ tons \end{aligned} \tag{26}$$

17- The 2010 Haiti nuclear earthquake and the 2023 Turkey-Syria nuclear earthquake may have been chosen to occur during the election period of the general elections and during a period of heavy rains to increase soil liquefaction and make more difficult rescue operations. The Haiti place may have been chosen to circumvent the United States embargo against Cuba by destabilizing neighboring countries (Cubans travel to Haiti searching for shopping bargains) and the Turkey-Syria place may have been chosen to reduce the number of Russian soldiers needed in Syria during the Ukraine war launched by Russia.

18- The natural earthquake in San Francisco 1906, the nuclear earthquake in Tangshan 1976 and the nuclear earthquake in Turkey–Syria 2023 have overturned few trains. HOWEVER, the train overturned by a natural earthquake in 1906 was ON the San Andreas fault (Figure 13).

19- The 2023 Turkey-Syria earthquake created a canyon 35 meters deep and 200 meters wide. It could be a land subsidence from the collapse of a very deep and very large cavity formed by an underground nuclear explosion (Figure 14).

20- The Russian international terrorism globally pushes to increase the use of contactless technologies, to increase the digitalization of human activities, to increase the redundancy of security standards and to raise the level of security standards.

21- Within the context of the 30 nuclear earthquakes about, the Chernobyl accident was fake and used for two purposes. The first one, to show a fake easily detectable unprofessional appearance with respect to the nuclear energy. The second one, to ensure a secrecy at an extremely high level within the Russian Federation by doing a PLANNED purge of political dissidents by sending them to deadly radioactive areas for unsafe decontamination work or by delaying their evacuations or giving them permanent jobs years ago in the Chernobyl region. The Russian Federation may have used some dirty nuclear activities as a "Final Solution" against political dissidents.

22- The Russian Federation may have created the LONG COVID disease as an attempt to globally reduce the intelligence of investigations about the 30 nuclear earthquakes about around the world that have struck dense urban areas near existing seismic faults (nuclear explosions are spatially arranged and temporally synchronized to reduce the Primary waves and to trigger the rupture of the existing seismic faults).

23- Perhaps, the next step in trying to make nuclear earthquakes forget is to detonate a few small nuclear bombs in Ukraine. It is a sketch already carefully decided in advance, the Russian army loses "too much" and is "forced" to use a few small tactical nuclear bombs in its "retirement". Everyone is obsessed with those potential events and no one is thinking at all about nuclear earthquakes.... who knows?

FIGURE 15. Nikita Sergeyevich Khrushchev had the Napoleon-complex?

REFERENCES

[1] A. Zaganidis, "Mathematica Notebooks and Pictures: A specific magnitude budget for the detection of 30 nuclear earthquakes in urban areas subject to an existing natural seismic hazard." https://drive.google.com/drive/folders/1Rid5ZDhbUKgQt1XHSdVGLiYODgAv5OAU?usp=share_link.

[2] J. Boatwright and G. Choy, "Teleseismic estimates of the energy radiated by shallow earthquakes (usa).," *Journal of Geophysical Research*, vol. 91, pp. 2095–2112, 02 1986.

[3] G. Choy and J. Boatwright, "Global patterns of radiated seismic energy and apparent stress," *Journal of Geophysical Research*, vol. 1001, pp. 18205–18228, 09 1995.

[4] H. Kanamori, "Chapter 11 energy budget of earthquakes and seismic efficiency," *International Geophysics*, vol. 76, pp. 293–305, 12 2001.

For a deep event, the energy radiated in the *P*- and *S*-waves can be estimated directly from measurements of the energy flux in the body-wave arrivals. Neglecting directivity, *Boatwright and Fletcher* [1984] derived the "point source" formulae

$$E_s^P = 4\pi\langle F^P\rangle^2\left(\frac{R^P}{F^P}\right)^2 \varepsilon_P^* \qquad (1a)$$

$$E_s^S = 4\pi\langle F^s\rangle^2\left(\frac{R^S}{F^{Si}}\right)^2 \varepsilon_{Si}^* \qquad (1b)$$

relating the total energy radiated in the body wave (E_s^P or E_s^S) to the energy flux contained in the *P*- or *S*-wave arrival.

MEASUREMENT OF THE ENERGY FLUX

As discussed by *Snoke et al.* [1983] and *Boatwright and Fletcher* [1984] for near-field data, the noise and the attenuation characteristics critically affect the correction of the "measured" energy flux. In this section, we consider how these factors condition the analysis of teleseismic data.

The energy flux in a plane wave can be calculated from the product of the density, the wave velocity, and the integral of the square of the ground velocity,

$$\varepsilon_c = \rho c \int_0^\infty \dot{u}_c^2(t)\, dt = \rho c I_c \qquad (16)$$

where the integration extends over the duration of the body-wave arrival. To correct this measurement for the attenuation suffered in the teleseismic propagation, Parseval's theorem can be used to replace the integral in equation (16) with an integral over angular frequency. The correction for the attenuation is determined using the function $t_c^*(\omega) = Q_c(\omega)/T_c$ in the integral over angular frequency:

$$\varepsilon_c^* = \frac{\rho c}{\pi}\int_0^\infty |\dot{u}_c(\omega)|^2 e^{\omega t_c^*(\omega)}\, d\omega = \rho c I_c^* \qquad (17)$$

For this analysis, we will use the description of $t_c^*(\omega)$ determined by *Der et al.* [1981, 1982, unpublished observations]. Their results are plotted in Figure 6, along with the approximation

$$t_\alpha^*(\omega) = 0.8 - 0.3 \ln_{10} f \qquad f < 1 \text{ Hz}$$
$$t_\alpha^*(\omega) = 0.8 - 0.7 \ln_{10} f \qquad f > 1 \text{ Hz} \qquad (18)$$

used to correct the energy flux measurements for the attenuation suffered on the Western U.S.–Shield paths.

In transforming from equation (16) to equation (17), the square of the time history of the ground velocity is replaced by the power spectrum of the ground velocity. The range of integration in equation (17) extends to infinite frequency. Unfortunately, the power spectrum of the ground velocity can be reliably determined only for a restricted frequency band. Figure 7 shows a comparison of the recorded signal-to-noise as a function of frequency for three of the *gP* waveforms radiated by the Borah Peak earthquake and the *gSH* waveform radiated by the Coalinga earthquake. The noise samples are taken from the data shown in Figures 2 and 4 using 30-s windows just before the body-wave arrivals. The *gP* spectra at stations

BOATWRIGHT AND CHOY: TELESEISMIC ESTIMATES OF RADIATED ENERGY 2101

radiation patterns. The seismic moment is then given by the relation,

$$M_0 = 4\pi\rho\alpha^3 \frac{R}{F^{gP}}\bar{u} \qquad (28)$$

The results of this analysis are compiled in Table 3; the average estimate of the seismic moment is $M_0 = (1.7 \pm 0.3) \times 10^{26}$ dyn cm, similar to the estimate of 1.7×10^{26} dyn cm estimated from the long-period GDSN data by S. A. Sipkin (personal communication, 1984) and $(1.85 \pm 0.16) \times 10^{26}$ dyn cm estimated from the long-period WWSSN body waves by *Barrientos et al.* [1985]. *Doser and Smith* [1985] estimated the moment as $1.6–2.1 \times 10^{26}$ dyn cm from a moment inversion of long period SRO data. We note that this is a long-period estimate, rather than a broad-band estimate, although the corner period of the Borah Peak earthquake ($\simeq 13$ s) is nearer to the 20-s period range than that of the Coalinga earthquake. Combining this moment with the radiated energy estimate corrected for the horizontal focussing of energy gives $\tau_a = 6.8 \pm 1.3$ bars.

KANAMORI: FRACTURE ENERGY OF EARTHQUAKES B05302

BDUCTING PLATE

f the different
lative to the

ed our results
cs.

ie

uakes relative
on zone earth-
late interface
interface be-

and 2001 (shown on the location map in Figure 2), we used *P* wave teleseismic data recorded at broadband stations around the world and archived at the IRIS Data Management Center. Only the vertical component data (BHZ channel) of stations at distances between 30° and 90° were used in this study. We applied corrections for path and radiation pattern [*Boatwright and Choy*, 1986], to determine the moment rate spectrum ($\dot{M}(f)$) from the displacement spectrum ($\hat{u}(f)$) at a station using

$$|\hat{\dot{M}}(f)| = \frac{4\pi\rho^3 v_{\alpha,\beta}^3 R_E e^{(\pi f t^*)}|\hat{u}(f)|}{g(\Delta)R(\theta,\phi)C|\hat{I}(f)|},$$

where at teleseismic distances the geometric spreading factor $1/r$ is replaced by $g(\Delta)/R_E$, $R_E = 6371$ km is the radius of the earth, $v_{\alpha,\beta}$ is the *P* wave or *S* wave velocity, t^* is the attenuation factor (equal to the travel time divided by the path-averaged *Q* factor), *C* is the free surface receiver effect, and $\hat{I}(f)$ is the instrument response. By integrating the squared moment rate spectrum determined at each station we computed radiated energy, E_R. Thus

$$E_R = \left[\frac{8\pi}{15\rho\alpha^5} + \frac{8\pi}{10\rho\beta^5}\right]\int_0^\infty f^2|\hat{\dot{M}}(f)|^2 df,$$

where ρ is the density, and α and β are the *P* and *S* wave velocities of the medium. We refer to this method of estimating radiated energy as the single-station method. The first and the second terms in the parenthesis on the right-hand side of the equation represent contributions from *P* and *S* waves, respectively; the *P* wave contribution is about 5 percent of the *S* wave contribution. The mean value of

FIGURE 16. The Energy Budget may have been used incorrectly in the following article: "Observational constraints on the fracture energy of subduction zone earthquakes" written by Venkataraman, Anupama and Kanamori, Hiroo in 2004 .

Location	Country	Days	Hypocentral Depth (km)	M_R	$M_R - M_{Work}$	E_R/E_{Work}	Costs (G$)
San Fernando 1971	United States	0.	8.4	6.21595	0.290465	2.72708	1.
Mexico 1985	Mexico	5335.97	23	8.19509	1.01269	33.0397	5
Whittier Narrows 1987	United States	6078.03	14	5.59023	0.293207	2.75302	0.4
Loma Prieta 1989	Mexico	6825.42	19	6.55138	0.356565	3.42647	6
Kushiro 1993	Japan	8010.88	100	7.22886	0.40558	4.05854	0.75
North Ridge 1994	United States	8377.94	18.2	6.87163	0.856365	19.2552	50
Great Hanshin 1995	Japan	8742.28	17.6	6.64467	0.449846	4.729	200
Jiji 1999	Taiwan	10 415.4	12	7.31835	0.45018	4.73445	10
Nisqually 2001	United States	10 977.2	57	6.51635	0.411308	4.13964	2
Geiyo 2001	Japan	11 000.7	50	7.31295	1.11813	47.5554	0.05
Southern Peru 2001	Peru	11 092.3	32	8.49382	0.952298	26.8192	0.75
Boumerdes 2003	Algeria	11 789.2	12	6.51251	0.40747	4.08513	5
Chuetsu 2004	Japan	12 309.8	13	6.98399	0.878946	20.817	28
Chuetsu 2007	Japan	13 305.5	10	6.00068	0.0752035	1.2966	12.5
Haiti 2010	Haiti	14 217.3	13	6.59832	0.313715	2.9551	8.5
Chile 2010	Chile	14 262.7	35	8.68125	0.780611	14.8223	30
Baja California 2010	Mexico	14 299.4	10	6.7133	0.249135	2.3643	1.1
Canterbury 2010	New Zealand	14 451.1	10	6.53246	0.15808	1.72631	40
Christchurch 2011	New Zealand	14 622.4	5	5.83651	0.315038	2.96864	40
Tohoku 2011	Japan	14 639.7	29	8.7112	0.631003	8.84107	720
Christchurch June 2011	New Zealand	14 733.5	7	5.90246	0.515659	5.93593	3
Northern Italy 2012	Italy	15 075.5	14.8	5.70731	0.230734	2.21871	15.8
Central Italy August 2016	Italy	16 632.5	19.2	6.32403	0.847449	18.6712	5
Chiappas 2017	Mexico	17 012.6	47.4	9.14434	1.87216	643.04	4
Osaka 2018	Japan	17 295.4	13	6.079	1.05132	37.7557	7
Hokkaido Eastern Iburi 2018	Japan	17 375.2	35	7.1917	1.26622	79.3101	2
Zagreb 2019	Croatia	17 938.6	10	5.05977	0.301432	2.83236	11.7
Fukushima 2021	Japan	18 267.	44	8.2392	1.86482	626.937	7.7
Fukushima 2022	Japan	18 663.	41	8.61102	2.05708	1217.9	4
Turkey-Syria 2023	Turquey	18 989.5	17.9	7.70835	0.7504	13.3536	100

FIGURE 17. Raw data of the 30 nuclear earthquakes.

[5] A. Venkataraman and H. Kanamori, "Observational constraints on the fracture energy of subduction zone earthquakes," *Journal of Geophysical Research: Solid Earth*, vol. 109, no. B5, 2004.

[6] J. Aubry, F. X. Passelègue, D. Deldicque, F. Girault, S. Marty, A. Lahfid, H. S. Bhat, J. Escartin, and A. Schubnel, "Frictional heating processes and energy budget during laboratory earthquakes," *Geophysical Research Letters*, vol. 45, no. 22, pp. 12,274–12,282, 2018.

[7] L. Serva, A. Blumetti, L. Guerrieri, and A. Michetti, "The apennine intermountain basins: The result of repeated strong earthquakes over a geological time interval," vol. 1, pp. 939–946, 01 2002.

Location	Country	Days	Hypocentral Depth (km)	M_R	$M_R - M_{Work}$	E_R / E_{Work}	Costs (G$)
Valdivia 1960	Chile	-3914.78	33	8.32841	-0.200687	0.5	8
Irpinia 1980	Italy	3575.19	10	5.87988	-0.314944	0.336964	15
Coalinga 1983	United States	4465.4	10	5.71767	-0.297592	0.357777	0.02
Borah Peak 1983	United States	4644.	16	5.69423	-0.500595	0.177463	0.02
Landers 1992	United States	7809.91	1.09	6.39077	-0.163174	0.569166	0.1
Izmit 1999	Turkey	10 450.2	15	6.45217	-0.371109	0.277547	20
Aquila 2009	Italy	13 935.5	9.46	5.85846	-0.336356	0.312943	16
Kaohsiung 2010	Taiwan	14 267.4	5	5.1475	-0.508639	0.1726	1
Kumamoto 2016	Japan	16 502.1	10	5.9028	-0.381798	0.267487	20
Puebla 2017	Mexico	17 024.2	54.5	6.07179	-0.392373	0.257893	8
Ridgecrest 2019	United States	17 678.6	8	5.86242	-0.511959	0.170632	5.3
Albania 2019	Albania	17 821.5	20	5.48553	-0.439948	0.218815	1
Petrinja 2019	Croatia	18 220.9	4.4	5.49763	-0.24829	0.424194	5
Haiti 2021	Haiti	18 448.9	10	6.05677	-0.407388	0.24486	1.5
Taitung 2022	Taiwan	18 848.7	7.3	5.59077	-0.604051	0.124143	0.147

FIGURE 18. Raw data of some 15 natural earthquakes.

[8] C. Perrin, F. Waldhauser, and C. Scholz, "The shear deformation zone and the smoothing of faults with displacement," *Journal of Geophysical Research Solid Earth*, vol. 126, pp. 1–18, 05 2021.

[9] T. G. S. H. A. P. (GSHAP). https://www.un-spider.org/links-and-resources/data-sources/global-seismic-hazard-assessment-gshap-icsu.

[10] S. Veeraraghavan, T. H. Heaton, and S. Krishnan, "Lower Bounds on Ground Motion at Point Reyes during the 1906 San Francisco Earthquake from Train Toppling Analysis," *Seismological Research Letters*, vol. 90, pp. 683–691, 01 2019.

[11] J. A. B. ume, "1976 tangshan, china earthquake (papers presented at the 2nd u.s. national conference on earthquake engineering held at stanford university)." https://nehrpsearch.nist.gov/static/files/NSF/PB82123175.pdf, August 22-24, 1979.

[12] L. Huixian, G. W. Housner, X. Lili, and H. Duxin, "The great tangshan earthquake of 1976," 2002.

[13] T. Imakiire and M. Koarai, "Wide-area land subsidence caused by "the 2011 off the pacific coast of tohoku earthquake"," *Soils and Foundations*, vol. 52, no. 5, pp. 842–855, 2012. Special Issue on Geotechnical Aspects of the 2011 off the Pacific Coast of Tohoku Earthquake.

[14] M. Matsubara, H. Sato, T. Ishiyama, and A. Van Horne, "Configuration of the moho discontinuity beneath the japanese islands derived from three-dimensional seismic tomography," *Tectonophysics*, vol. 710-711, pp. 97–107, 2017. Evolution of fore-arc and back-arc sedimentary basins with focus on the Japan subduction system and its analogues.

[15] J. Patton, "Violent shaking triggers massive landslides in sapporo japan earthquake." https://static.temblor.net/wp-content/uploads/2018/09/M66_figure_02_geology_plate_boundaries_blue_star-910x1024.jpg, September 6, 2018.

[16] Wikipedia. https://en.wikipedia.org/wiki/Seismic_magnitude_scales.

[17] Wikipedia. https://wiki.seg.org/wiki/Seismic_attenuation.

[18] Wikipedia. https://en.wikipedia.org/wiki/List_of_costliest_earthquakes.

[19] Wikipedia. https://en.wikipedia.org/wiki/List_of_megathrust_earthquakes.

[20] Wikipedia. https://en.wikipedia.org/wiki/1906_San_Francisco_earthquake.

[21] Wikipedia. https://en.wikipedia.org/wiki/Nikita_Khrushchev.

[22] Wikipedia. https://en.wikipedia.org/wiki/Sino-Soviet_split.

[23] Wikipedia. https://en.wikipedia.org/wiki/Gyrotron.

[24] Wikipedia. https://en.wikipedia.org/wiki/Cuban_Missile_Crisis.

[25] Wikipedia. https://en.wikipedia.org/wiki/Kola_Superdeep_Borehole.

[26] Wikipedia. https://en.wikipedia.org/wiki/Helsinki_Accords.

[27] Wikipedia. https://en.wikipedia.org/wiki/1975_Banqiao_Dam_failure.

[28] Wikipedia. https://en.wikipedia.org/wiki/1976_Tangshan_earthquake.

[29] Wikipedia. https://en.wikipedia.org/wiki/1983_Coalinga_earthquake.

[30] Wikipedia. https://en.wikipedia.org/wiki/1983_Borah_Peak_earthquake.

[31] Wikipedia. https://en.wikipedia.org/wiki/1985_Mexico_City_earthquake.

[32] Wikipedia. https://en.wikipedia.org/wiki/1987_Whittier_Narrows_earthquake.

[33] Wikipedia. https://en.wikipedia.org/wiki/1992_Landers_earthquake.

[34] Wikipedia. https://en.wikipedia.org/wiki/1993_Kushiro_earthquake.

[35] Wikipedia. https://en.wikipedia.org/wiki/1994_Northridge_earthquake.

[36] Wikipedia. https://en.wikipedia.org/wiki/Great_Hanshin_earthquake.

[37] Wikipedia. https://en.wikipedia.org/wiki/2001_Nisqually_earthquake.

[38] Wikipedia. https://en.wikipedia.org/wiki/2001_Geiyo_earthquake.

[39] Wikipedia. https://en.wikipedia.org/wiki/2001_southern_Peru_earthquake.
[40] Wikipedia. https://en.wikipedia.org/wiki/2010_Haiti_earthquake.
[41] Wikipedia. https://en.wikipedia.org/wiki/2010_Kaohsiung_earthquake.
[42] Wikipedia. https://en.wikipedia.org/wiki/2011_Tokohu_earthquake_and_tsunami.
[43] Wikipedia. https://en.wikipedia.org/wiki/2017_Chiapas_earthquake.
[44] Wikipedia. https://en.wikipedia.org/wiki/2019_Ridgecrest_earthquakes.
[45] Wikipedia. https://en.wikipedia.org/wiki/2022_Taitung_earthquakes.
[46] Wikipedia. https://en.wikipedia.org/wiki/2023_Turkey%E2%80%93Syria_earthquake.
[47] Youtube, "Cubans travel to haiti searching for shopping bargains." https://www.youtube.com/watch?v=oQR7VidXBA4, 2018.
[48] Wikipedia. https://en.wikipedia.org/wiki/Shear_modulus.